

Synthesis and characterization of $\text{GdVO}_4:\text{Dy}^{3+}$ nanosheets as down converter: application in dye-sensitized solar cells

M. Zahedifar^{1,2} · Z. Chamanzadeh² · M. Madani² · M. Moradi² · N. Sharifpour²

Received: 29 September 2015 / Accepted: 10 January 2016 / Published online: 23 January 2016
© Springer Science+Business Media New York 2016

Abstract The effect of $\text{GdVO}_4:\text{Dy}^{3+}$ luminescent film as down converter material on the efficiency of dye sensitized solar cell (DSSC) was investigated. For this purpose, GdVO_4 nanoparticles doped with lanthanide were synthesized by hydrothermal method and the effect of different parameters such as temperature, reaction time, concentration of dopant and annealing regime on their morphology and photoluminescence (PL) properties were studied. The ultraviolet–visible (UV–Vis) and PL spectroscopy studies indicated that GdVO_4 nanoparticles could be used as luminescent down conversion (DC) and UV filters. Considering the decrease of chemical stability of dye sensitized solar cells under UV radiation, nanoparticles of $\text{GdVO}_4:\text{Dy}^{3+}$, constructed as a UV filter and the luminescent DC were used to increase the cell efficiency of DSSC. The efficiency of DSSC increased by 10.30 % using a film of nanoparticles on the back surface of the photo electrode (PE) and by 2.69 %, when the nanoparticles were used to prepare the PE of DSSC, compared with a DSSC lacking $\text{GdVO}_4:\text{Dy}^{3+}$.

1 Introduction

Currently, dye-sensitized solar cells (DSSCs) have attracted much attention for their practical application as a promising candidate for the development of next gen-

eration solar cells because of their low fabrication cost and relatively high efficiency [1–6]. However, how to enhance its efficiency is still a crucial problem. In general, the cell consists of a porous nanocrystalline TiO_2 film sensitized by a dye for absorbing incident light, a redox electrolyte, and a platinized counter electrode to catalyze the redox couple regeneration reaction [3, 7]. To improve the harvest of incident light and increase the photocurrent of the DSSC, many dyes have been synthesized. However, even the best (N-719, N-749) of these absorb only visible light in the wavelength range 300–800 nm [3, 7].

For the practical use of DSSCs, the chemical stability is as important as its conversion efficiency. Irreversible electrochemical and thermal degradation of the dye or electrolyte components, originating from UV irradiation affect the chemical stability of DSSCs [8, 9]. An effective way to reduce the energy losses is modifying the solar energy spectrum via luminescence phenomenon to the wavelength range in which the solar cells have high absorption probability [9, 10]. The solar spectrum modification results in efficiency enhancement of solar cell through down shifting (DS), down conversion (DC) and up conversion (UC) [9].

Rare earth (RE) doped luminescence materials are of significance for their wide potential applications as anode materials in lithium ion batteries, ferroelectrics, laser host materials, luminescent materials [11] and down converters in dye sensitized solar cells (DSSCs) [9]. Common strategy to avoid the UV light is using an additional UV filter specially coated to absorb ultraviolet light. The gadolinium orthovanadate (GdVO_4) rare-earth doped luminescence nanocrystals (NCs) are among the most important functional materials, which can act as UV filter [12]. Synthesis of GdVO_4 powders has been previously accomplished using high-temperature solid state reaction between Gd_2O_3

✉ M. Zahedifar
zhdf@kashanu.ac.ir

¹ Physics Department, Faculty of Physics, University of Kashan, Kashan, Iran

² Institute of Nanoscience and Nanotechnology, University of Kashan, Kashan, Iran

and NH_4VO_3 [12]. Hydrothermal method is amongst the most promising solution chemical methods, in which the particle size and distribution, phase homogeneity, and morphology can be well-controlled [13]. By far, GdVO_4 nanoparticles (NPs) of different shapes, such as wire like, rod like and cube like have been successfully synthesized by the hydrothermal method [14–16]. These works bring us lots of interesting results and fabrication techniques. Among lanthanide doped GdVO_4 NPs, Dy-doped GdVO_4 have attracted a great deal of interest [17, 18].

Due to capability to absorb the UV light and emit the visible light, employing $\text{GdVO}_4:\text{Dy}^{3+}$ as down converter material, increases the chemical stability of DSSC. Making use of this material in outer surface of DSSC, causes reflection of the incoming light. Since the photoluminescent materials usually have a refractive index in the range between 1 and 10, more than half of the PL emission is lost in the sun direction, resulting in a net loss of light current generated by the solar cell instead of an increase and therefore there is possibility of decrease of the photocurrent in DSSC [19].

Sheet-like $\text{GdVO}_4:\text{Dy}^{3+}$ NPs were successfully fabricated via a simple hydrothermal method. The as-prepared samples were characterized by using powder X-ray diffraction (XRD), scanning electron microscopy (SEM), UV–vis diffuse reflectance spectroscopy (UV–vis) and PL spectroscopy. For the first time, the effect of the produced nanostructures as down conversion film on the efficiency of DSSC was investigated. In order to retain the energy of UV light and yet keep up the chemical stability of DSSC, the use of $\text{GdVO}_4:\text{Dy}^{3+}$ NPs as a PE of DSSC can be a suitable strategy, since the absorption of reflected photons by DC material increases the photocurrent of DSSC by photoanode.

2 Experimental

2.1 Synthesis of GdVO_4 nanoparticles

Chemical reagents including Gadolinium (III) nitrate hexahydrate ($\text{Gd}(\text{NO}_3)_3 \cdot 6\text{H}_2\text{O}$, Aldrich), Dysprosium (III) nitrate pentahydrate ($\text{Dy}(\text{NO}_3)_3 \cdot 5\text{H}_2\text{O}$, Alfa Aesar), ammonium metavanadate (NH_4VO_3 , Merck), Ethanol (Merck), Oleic acid (Merck), NaOH (Merck), deionized (DI) water (Merck) were analytical reagents. $\text{GdVO}_4:\text{Dy}^{3+}$ nanoparticles were prepared using the simple hydrothermal method. In a typical synthesis, a solution of 5.5 ml deionized water containing 0.03 g of NH_4VO_3 and 0.3 g of NaOH form a Na_3VO_4 aqueous solution. 10 ml surfactant solution containing Oleic acid and Ethanol with proportion of 1:1 was slowly added to initial solution. Then a solution of 0.22 g precursor of $\text{Gd}(\text{NO}_3)_3 \cdot 6\text{H}_2\text{O}$ and $\text{Dy}(\text{NO}_3)_3 \cdot$

$5\text{H}_2\text{O}$ (1 mmol total) in 1 ml deionized water were slowly added to the above solution at room temperature, while was stirred for 15 min. The mixture was transferred to a 50 mL autoclave and maintained at 160 °C for 12 h. When the autoclave was cooled to room temperature naturally, white precipitate was obtained. The precipitate was washed with ethanol, centrifuged and dried at 60 °C in air. Then, GdVO_4 nanoparticles with different molar ratios of Dy^{3+} ion were synthesized by the above mentioned method and the effect of various parameters such as temperature, synthesis duration and annealing procedure on the morphology and PL properties were studied. The synthesis temperature and duration for 6 produced samples are shown in Table 1.

2.2 Fabrication of DSSCs

Electrophoresis deposition (EPD) was utilized to prepare working electrode used in DSSCs. EPD solution was prepared by mixing TiO_2 nanopowders (P25), acetone, acetyl acetone, I_2 , DI water, and ethanol. This mixture was stirred for 24 h. During EPD, the cleaned FTO glass maintained at a positive potential (anode) while a pure steel mesh was used as the counter (cathode) electrode. The distance between the two electrodes was about 1 cm with an applied voltage of 10 V. Six deposition cycles, each with duration of 5 s were accomplished. The coated substrates were dried at 150 °C in air for 5 min. The thickness of the resulting layer was 15 μm and heat-treated at 500 °C in air for 15 min. For sensitizing, the working electrodes were immersed in a solution of N719 dye in ethanol and acetonitrile (0.03 mM) for 24 h. Counter electrode was prepared by spin coating of a solution of H_2PtCl_6 on the FTO glass. Two electrodes with a spacer film of Surlyn were joined together then the electrolyte containing I^-/I_3^- redox couple was injected into the cell.

The effect of $\text{GdVO}_4:\text{Dy}^{3+}$ NPs as down converter material on the performance of DSSC was investigated through two ways. Firstly, a uniform thin film of $\text{GdVO}_4:\text{Dy}^{3+}$ NPs at 0.1 and 0.3 M concentration in cyclohexene was prepared by spin coating method at 3000 rpm for 30 s on the back surface of working electrode and secondly, these NPs introduced into the EPD solution as impurity with different molar ratios in initial layers of working electrode.

2.3 Characterization

X-ray diffraction (XRD) patterns were recorded by a Philips- X'Pert Pro, X ray diffractometer using Ni-filtered Cu K_α radiation at scan range of 2θ (0–70). Scanning electron microscope (SEM) and energy dispersive analysis of X-ray (EDAX) were taken by MIRA 3 FEG Tescan. Room

Table 1 Reaction conditions for GdVO₄:Dy³⁺ NPs

Sample No.	Temperature (°C)	Time (h)	Sample No.	Temperature (°C)	Time (h)
1	140	12	4	160	12
2	160	4	5	160	24
3	160	8	6	180	12

temperature PL (PL) was studied on a Perkin-Elmer (LS 55) fluorescence spectrophotometer. UV–Vis diffuse reflectance spectroscopy analysis (UV–Vis) was measured using Shimadzu UV–Vis scanning spectrometer. The photovoltaic measurements were accomplished by solar simulator (Luzchem) and IVIUMSTAT (IVIUM) under AM 1.5 condition. For measurement of thickness of working electrode a 3D Optical Microscopy Nanofocus was used.

3 Results and discussion

3.1 Structure and morphology

X-ray powder diffraction (XRD) patterns of GdVO₄ and GdVO₄:Dy³⁺ nanoparticles at room temperature are shown in Fig. 1. The sharp peaks of this sample at 18°, 24°, 33°, 35°, 49° and 50° can be perfectly assigned to [101], [200], [112], [220], [312] and [213] planes of the tetragonal phase of GdVO₄ with lattice constants comparable to the values

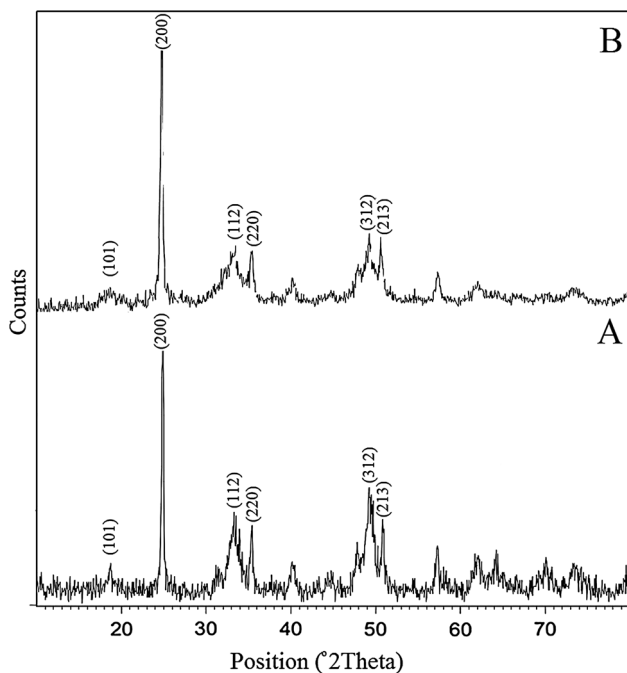


Fig. 1 XRD patterns of a GdVO₄ and b GdVO₄:Dy³⁺ NPs

given in JCPDS 72-0277. No impurity traces were detected, indicating that the product is rather pure. The sharp peaks in XRD pattern indicate the crystalline phase of the sample with the lattice constants of a = b = 7.19 Å and c = 6.33 Å. From XRD data the crystallite size of the as-prepared GdVO₄:Dy³⁺ nanocrystal was calculated to be 10–60 nm using the Scherer equation:

$$D_c = \frac{K\lambda}{\beta \cos \theta}$$

where β is the width of the observed diffraction line at its half intensity maximum, K is the so-called shape factor, which usually takes a value of about 0.9, and λ is the wavelength of X-ray source used in XRD.

EDAX analysis was employed to investigate the chemical composition of as-synthesized GdVO₄:Dy³⁺ nanocrystalline. EDAX pattern shown in Fig. 2 confirms that Gd, V and O are the major chemical components with approximate atomic ratios of 12.11, 13.02 and 70.10 % respectively. The concentration of Dy is about 0.65 %. The presence of C with concentration of 4.12 % is due to absorption of CO₂ from the precursors. The morphology and structural details of GdVO₄ nanoparticles are shown in Fig. 3. From the SEM micrograph, we can observe that the as-prepared samples are

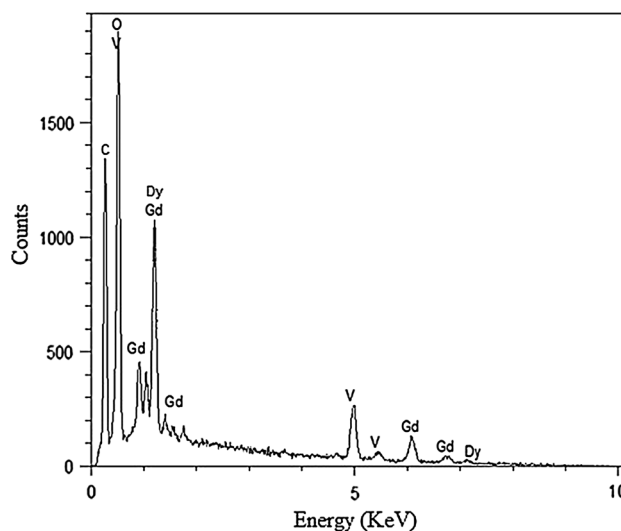


Fig. 2 EDX pattern of GdVO₄:Dy³⁺ NPs

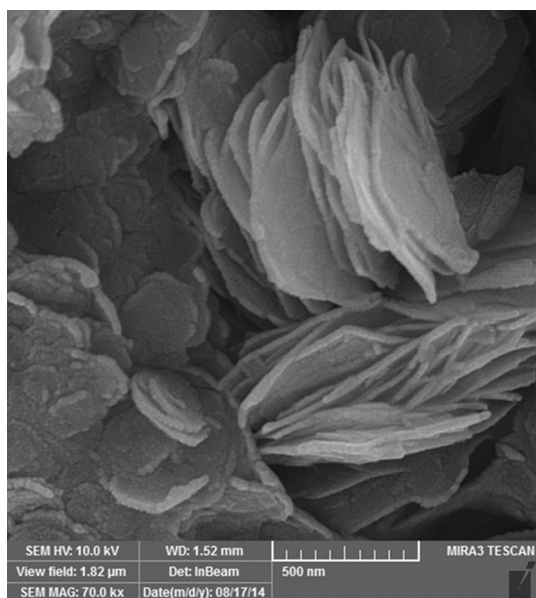


Fig. 3 SEM images of the as prepared GdVO_4 NPs

composed of square shaped nanosheets. As seen, thickness of these nanosheets is about 30 nm.

The influence of time and temperature of synthesis on morphology of $\text{Gd}_{0.98}\text{VO}_4:\text{Dy}_{0.02}$ were also studied. Figure 4 indicates the XRD pattern of prepared $\text{GdVO}_4:\text{Dy}^{3+}$ at different time and temperature. It is shown the GdVO_4 pattern with tetragonal phase for all of the samples. Figure 5 shows the SEM images of samples prepared according to Table 1. As is seen, nanosheets prepared at 140 and 180 °C are agglomerated in Fig. 5a, f. Comparing Figs. 5b–e, it is clear that the sample 4, prepared at 160 °C for 12 h has better morphology.

On the basis of the results above, the formation of GdVO_4 nanosheets demonstrated with a possible growth process, as shown schematically in Fig. 6. The oleic acid molecules control the growth of the nanocrystalline particles with formation micelle structures in aqueous solution and ethanol is a component producer of the micelle system. In micelle system, the inner chambers of micelles act as a template and are caused regular structures and special morphologies [20]. During the reaction process, the NH_4VO_3 first reacted with NaOH to form Na_3VO_4 solution. VO_4^{3-} anions trapped in the micelle chambers. So the subsequently added Gd^{3+} ions have a greater chance of reacting with VO_4^{3-} and under treatment in the oven, the reaction process will be completed. As seen in Fig. 6, the particles growth were restricted in one dimension, so the growth occurred in two other dimensions. Thus, the sheet-like morphology were obtained.

For clarifying the effect of annealing regime on XRD pattern, $\text{Gd}_{0.98}\text{VO}_4:\text{Dy}_{0.02}$ NPs were annealed at 300, 500 and 700 °C for 1 h. Figure 7 indicates the tetragonal phase

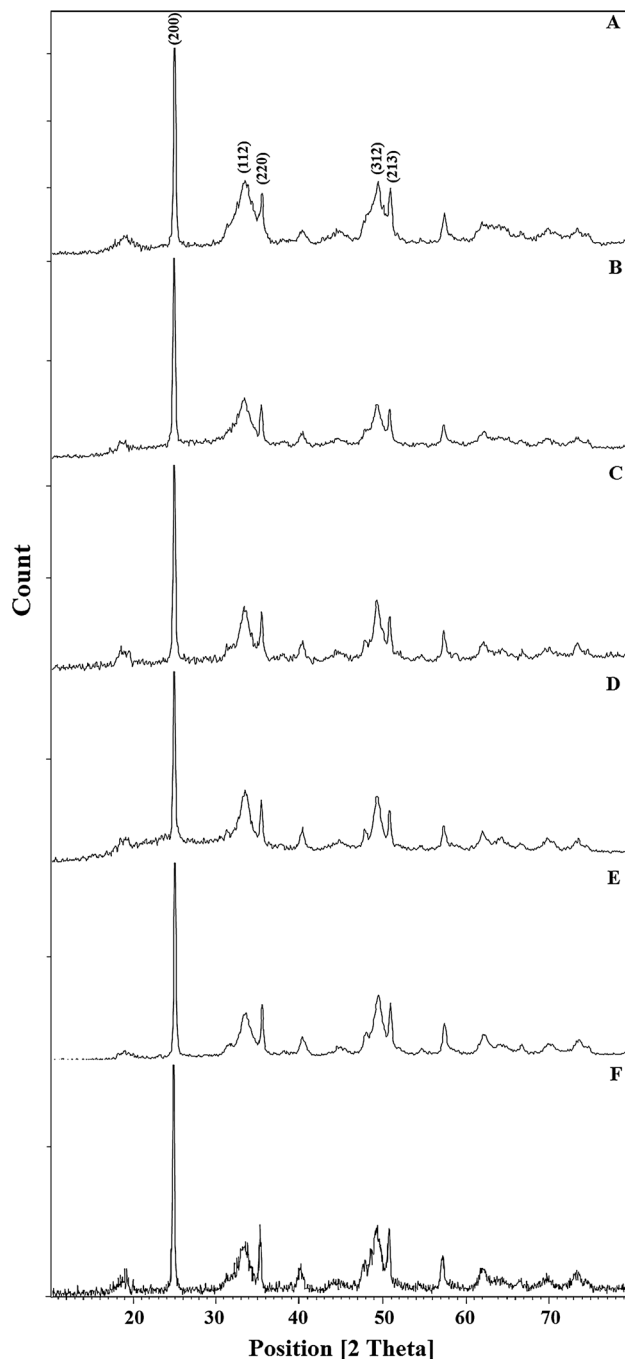
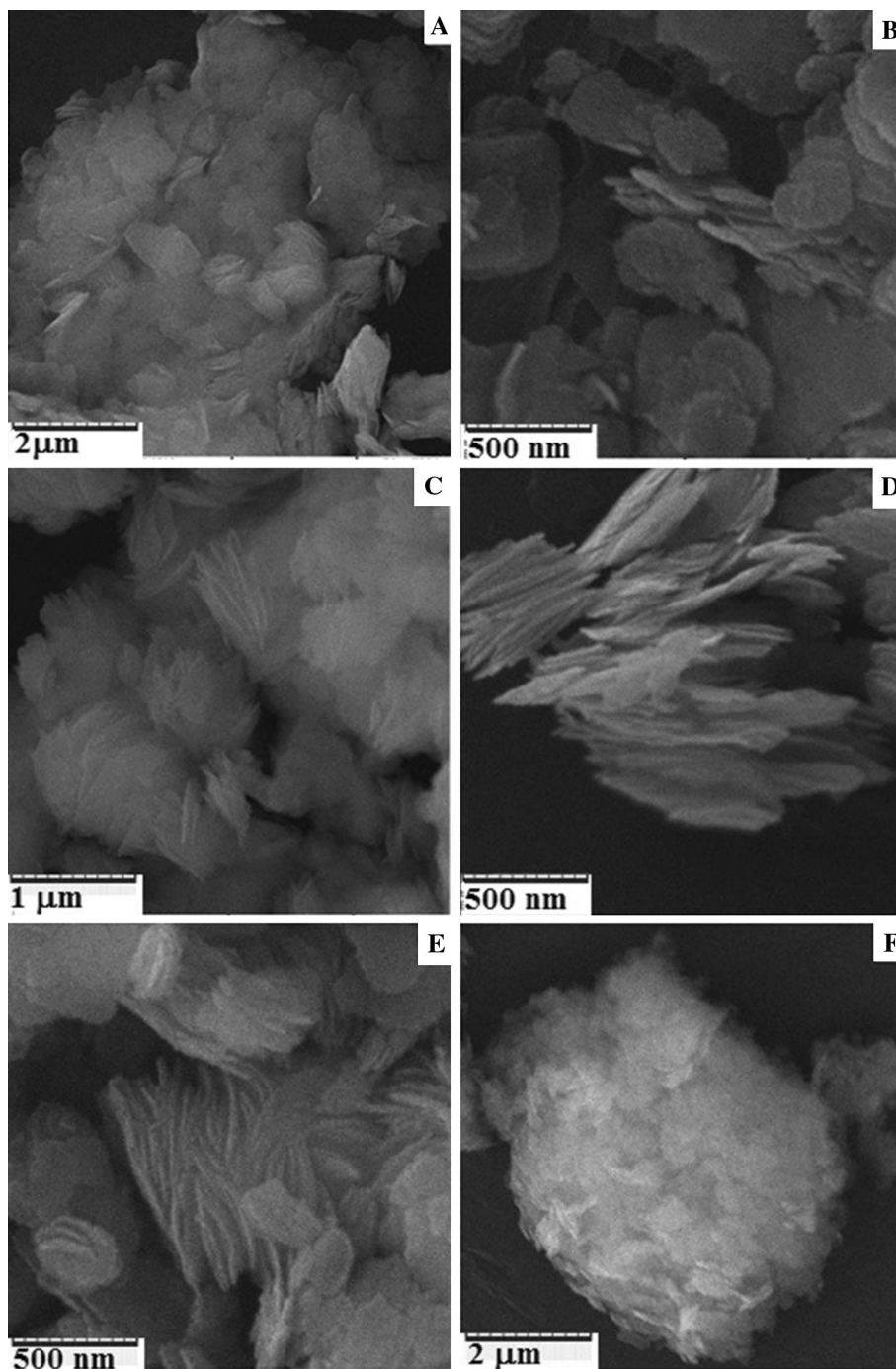


Fig. 4 XRD patterns of the samples prepared at a 140 °C, 12 h; b 160 °C, 4 h; c 160 °C, 8 h; d 160 °C, 12 h; e 160 °C, 24 h; f 180 °C, 12 h

of GdVO_4 which can be fitted with JCPDS Card no.72-0277. The peak intensity becomes stronger with increase in temperature from 300 to 500 °C implying better crystallinity. But this peak intensity was decreased in temperature from 500 to 700 °C due to increase of amorphous phase. So increase of temperature is not suitable because of eventuality phase change or oxidation of NPs.

Fig. 5 SEM images of $\text{GdVO}_4:\text{Dy}^{3+}$ NCs prepared at **a** 140 °C, 12 h; **b** 160 °C, 4 h; **c** 160 °C, 8 h; **d** 160 °C, 12 h; **e** 160 °C, 24 h; **f** 180 °C, 12 h



3.2 Optical properties

The room temperature UV–Vis diffuse reflectance spectra of the $\text{GdVO}_4:\text{Dy}^{3+}$ sample is presented in Fig. 8a. As shown in Figure, this sample could absorb UV light with the maximum absorption at 285 nm and is transparent for visible light. Therefore, the addition of GdVO_4 film would reduce the UV absorption of DSSCs and the lifetime of

DSSCs could be greatly enhanced due to the filtering of UV light. Since the light absorption relates to the host lattice, this analysis describes GdVO_4 without impurity [21].

The optical band gap of the NPs was determined from the optical absorption spectra. The optical absorption of the NPs shows a sudden increase at around 285 nm. However, a more accurate estimate of the band gap E_g was made by

Fig. 6 Schematic diagram showing the formation of $\text{GdVO}_4:\text{Dy}^{3+}$ nanosheets

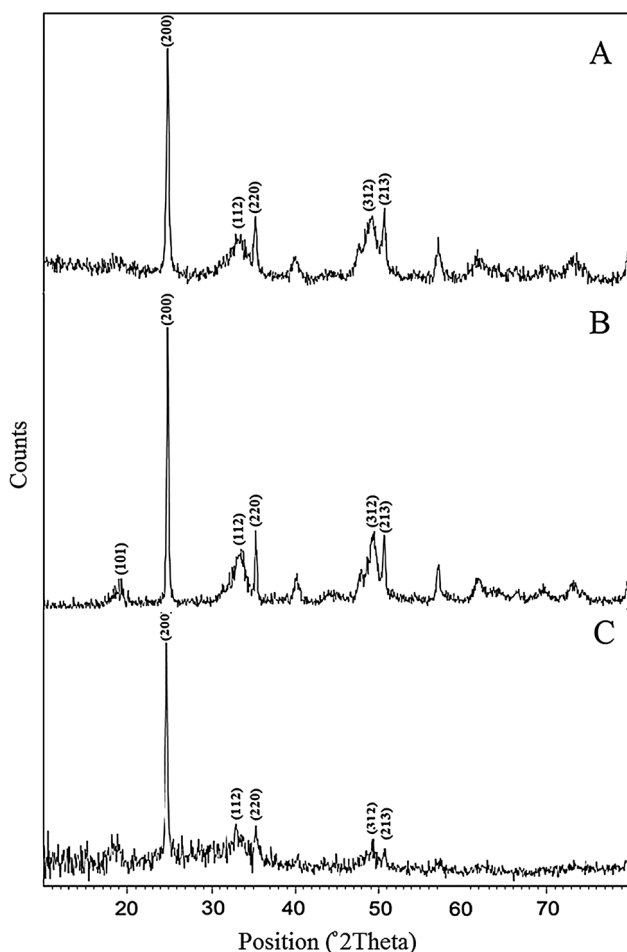
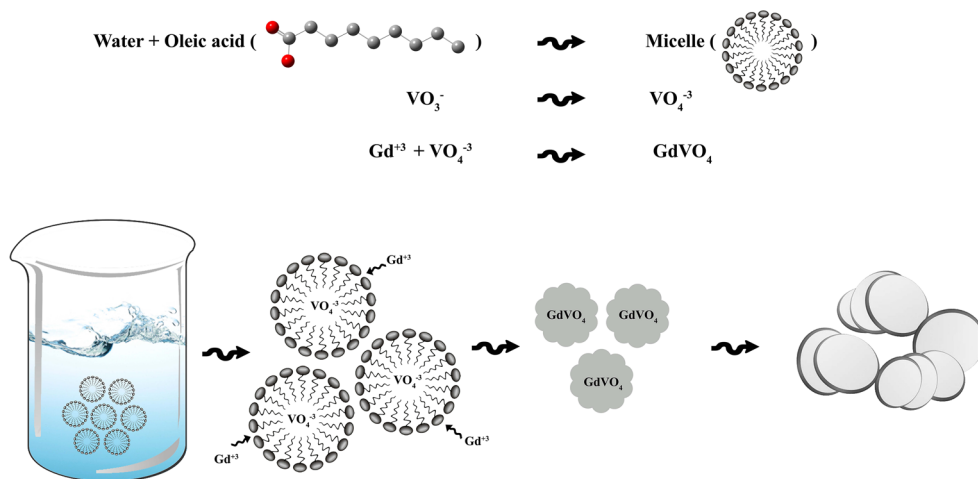


Fig. 7 XRD patterns of the samples annealed at temperature: *a* 300, *b* 500, *c* 700 °C

assuming a direct transition between valence band and conduction band [22]. The absorption coefficient α is related to the band gap E_g as:

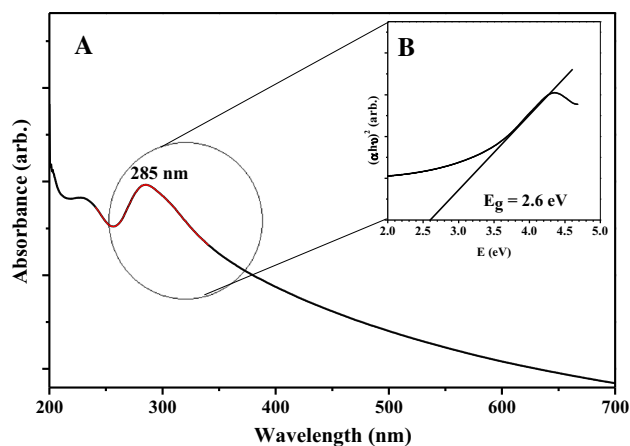


Fig. 8 *a* The absorption spectra of GdVO_4 NPs, *b* extrapolating the linear portion of the plot $(\alpha h\nu)^2$ versus $h\nu$ to $(\alpha h\nu)^2 = 0$ that determines the optical band gap E_g

$$\alpha h\nu = B(h\nu - E_g)^{1/2} \quad (1)$$

where $h\nu$ is the energy of the photon. The absorption coefficient α has been calculated from the optical absorption using the relation $\alpha = (1/t) \log(\text{absorption})$. The optical band gap E_g was determined by extrapolating the linear portion of the plot relating $(\alpha h\nu)^2$ and $h\nu$ to $(\alpha h\nu)^2 = 0$ [23]. Therefore, according to Fig. 8b the value of 2.6 eV was obtained for the E_g .

PL spectroscopy is important to characterize the optical properties. The effect of concentration of Dy^{3+} ion as impurity on the PL property was investigated. The room temperature PL spectra of GdVO_4 NPs and $\text{Gd}_{1-x}\text{VO}_4:\text{Dy}_x$ ($x = 0, 0.01, 0.02, 0.04, 0.06, 0.08$) NPs dispersed in cyclohexane and for excitation wavelength of 285 nm are shown in Fig. 9. According to the emission spectra, PL spectra of GdVO_4 NPs show weak emission in 450–550 nm, But the PL spectra of $\text{GdVO}_4:\text{Dy}^{3+}$

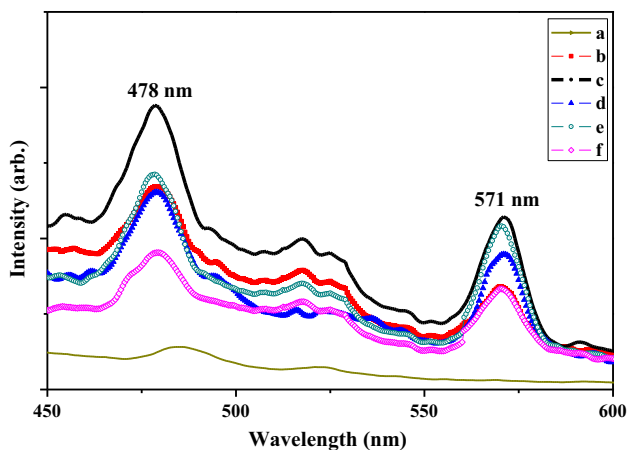


Fig. 9 The emission spectra of $Gd_{1-x}VO_4:Dy_x^{3+}$: a $x = 0.00$, b $x = 0.01$, c $x = 0.02$, d $x = 0.04$, e $x = 0.06$, f $x = 0.08$

nanosheets have strong peaks at 478 and 571 nm. Therefore, the presence of Dy ions as impurity in lattice site of $GdVO_4$ NPs causes the intensity of PL spectra to increase. Figure 10 shows the PL intensity of $GdVO_4:Dy^{3+}$ nanosheets as a function of impurity concentration. According to the emission spectra, the PL intensity of $Gd_{1-x}VO_4:Dy_x$ is optimized in 0.02 mmol impurity concentration.

Excitation with wavelength of 285 nm leads to partial electron transfer from the excited states of $[VO_4]^{3-}$ to the $^4F_{9/2}$ band of Dy^{3+} . This process involves fast multiphonon assisted non-radiative (NR) relaxation processes in Dy^{3+} . Subsequently, Dy^{3+} emits visible photons peaking at 478 and 571 nm respectively, due to transitions from $^4F_{9/2}$ to 6H_J ($J = 15/2, 13/2$) [12]. Figures 11 and 12 show the PL spectra of $Gd_{0.98}VO_4:Dy_{0.02}$ NPs prepared at various synthesis durations and temperatures in accordance with

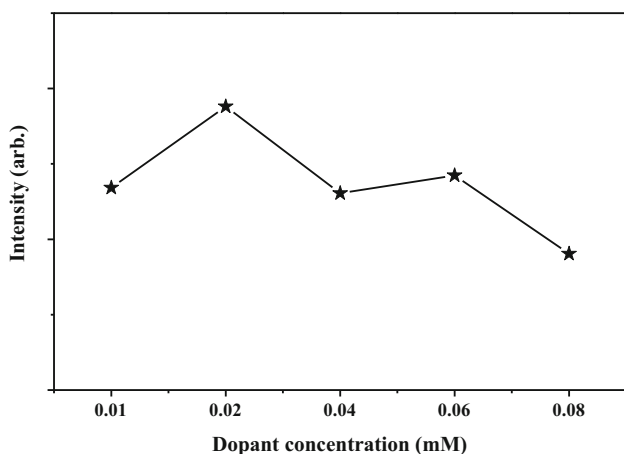


Fig. 10 The PL emission intensity of $GdVO_4:Dy^{3+}$ nanosheets as a function of dopant concentration

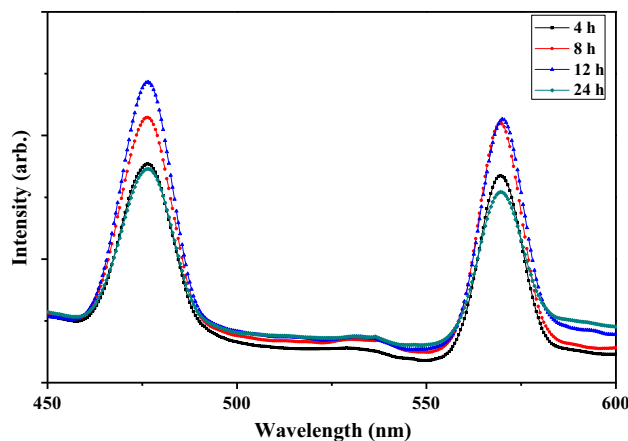


Fig. 11 The emission spectra of $Gd_{0.98}VO_4:Dy_{0.02}$ NPs prepared in various time at temperature of 160 °C

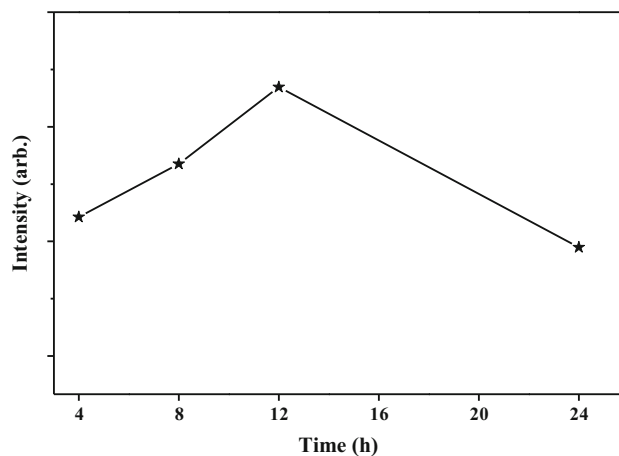


Fig. 12 The PL intensity of $GdVO_4:Dy^{3+}$ nanosheets as a function of production time

Table 1. As is evident, the sample synthesized at 160 °C for 12 h has maximum PL intensity. Therefore, both the PL spectra and SEM results confirm that the optimized synthesis condition for temperature and time are 160 °C and 12 h.

Figure 13 displays the PL spectra of samples annealed at different temperatures and under excitation at 285 nm. As shown in Fig. 13, a small shift to longer wavelengths is evident compared with the non-annealed sample. Also, with raising the annealing temperature from 300 to 500 °C, the emission intensity increases as a result of improved crystallinity and decrease in inherent lattice defects [24]. By further raising the temperature from 500 to 700 °C, the PL spectra decreased due to diminish of crystallinity. However, the PL spectra of non-annealed sample is sharper than those of the annealed samples. Therefore, PL studies confirm that the $Gd_{0.98}VO_4:Dy_{0.02}$ NPs is a good choice for use in DSSC as DC material.

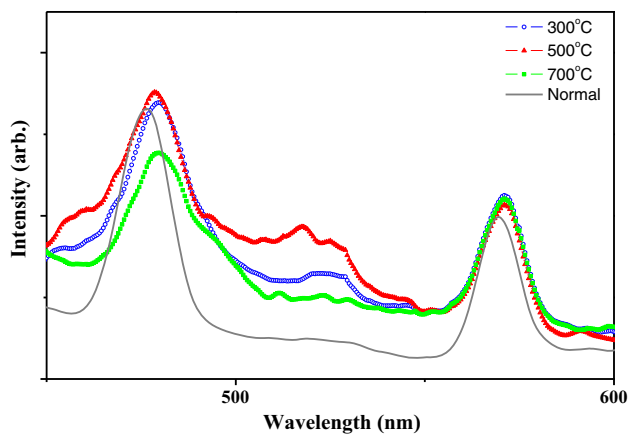


Fig. 13 The emission spectra of $\text{Gd}_{0.98}\text{VO}_4:\text{Dy}_{0.02}$ NPs annealed at different temperatures

3.3 Photoelectric performance of DSSCs with different PEs

To investigate the effect of a down converter material on the DSSC, the optimized $\text{Gd}_{0.98}\text{VO}_4:\text{Dy}_{0.002}$ NPs (synthesized at 160 °C, 12 h) were used. Figure 14 depicts the photocurrent–voltage characteristics of DSSCs for PE without $\text{GdVO}_4:\text{Dy}^{3+}$ NPs and with different concentration of $\text{GdVO}_4:\text{Dy}^{3+}$. The results are summarized in Table 2.

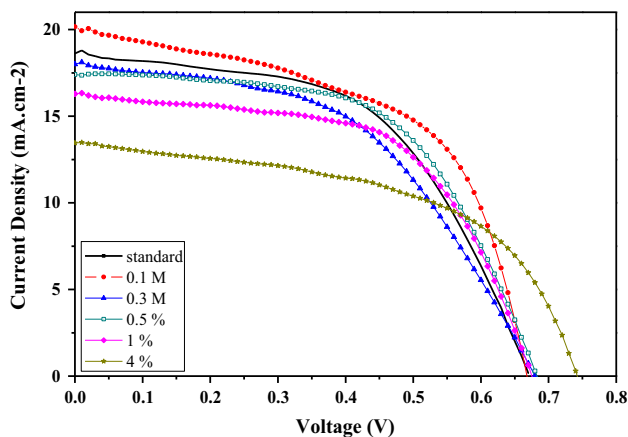


Fig. 14 The photocurrent–voltage curves of the fabricated dye-sensitized solar cells

Table 2 Photovoltaic characteristics of the fabricated DSSCs

Device No.	Condition	Concentration	J_{sc} (mA/cm ²)	V_{oc} (V)	FF	η (%)
1	Standard	–	18.62	0.67	0.54	6.70
2	Back surface of the PE	1 mM	20.16	0.67	0.55	7.39
3	Back surface of the PE	3 mM	18.19	0.69	0.49	6.14
4	Used to prepare the PE	0.5 %	17.40	0.68	0.58	6.88
5	Used to prepare the PE	1 %	16.29	0.68	0.58	6.39
6	Used to prepare the PE	4 %	13.45	0.75	0.53	5.33

The uncoated solar cell had a short current density (J_{sc}) of 18.62 mA.cm⁻², fill factor (FF) of 0.54, open circuit voltage (V_{oc}) of 0.67 V and with energy efficiency of 6.70 %. Accordingly, the solar cell coated with luminescent film with concentration of 0.1 M, had J_{sc} of 20.16 mA cm⁻², FF of 0.55, V_{oc} of 0.67 V and efficiency of 7.39 %. So, the solar cell coated with luminescent film with concentration of 0.1 M improved the current density and energy conversion efficiency by 8.28 and 10.30 %, respectively. This is because the emitted light by down-converter can be reabsorbed by N719 dye and generates current. Presence of $\text{GdVO}_4:\text{Dy}^{3+}$ NPs on the surface of DSSC causes the incoming single photons from UV to be converted to two visible photons [10, 12, 25]. This mechanism results in an increase of photon flux and finally an increase in current density which eventually improves the efficiency.

But the current density and energy conversion efficiency in a solar cell coated with luminescent film with concentration of 0.3 M, are reduced respectively to 2.31 and 8.36 % since by increase concentration, the possibility of reflection of incoming light is enhanced. The above obtained result and the possibility of cleaning DC material on cell surface encouraged us to use this material in PE of DSSC and near to the cell surface.

According to the data in Table 2, the DSSC efficiency for the samples with concentrations more than 1 % of DC material are decreased because of exceeding replacement of $\text{GdVO}_4:\text{Dy}^{3+}$ with TiO_2 that causes reduction in dye absorption by TiO_2 NPs and rise in recombination of charge carriers due to different morphology of TiO_2 NPs and DC NPs.

Therefore, by decrease of concentration of DC NPs to 0.5 %, photovoltaic characteristics were obtained as J_{sc} of 17.40 mA.cm⁻², FF of 0.58, V_{oc} of 0.68 V and η of 6.88 % according to Table 2. Therefore PE with 0.5 % concentration of DC NPs improved the FF and energy conversion efficiency by 7.41 and 2.69 %. This increase of fill factor due to increase in J_{mpp} , causes an enhancement in efficiency of DSSC. If the concentration of DC material is lower than 0.5 %, the influence of the UV filter is lost.

A decrease in overall energy efficiency has been reported for a DSSC coated with a film consisting

LaVO₄:Dy³⁺ NCs prepared by a Lanthanum source [26]. In other research, a DSSC with Eu³⁺ doped TiO₂ nanorods as down converter material was fabricated in a bilayer electrode of Eu³⁺ doped TiO₂ nanorod/TiO₂ nanoparticle (Eu-NR/NP) [27]. An increase in light-to-electrical energy conversion efficiency by 1 % has been reported for a cell including Eu-NR/NP bilayer electrode compared with the cell consisting un-doped bilayer electrode. Increase of current density and energy conversion efficiency respectively by 6.7 and 2.6 % was reported for DSSC solar cell coated with LaVO₄:Dy NPs as down converter material [9]. Considering the results obtained in this work, the synthesized GdVO₄:Dy NPs is recommended as down-conversion material and UV filter for DSSCs.

4 Conclusion

The presence of Dy ion as impurity in GdVO₄:Dy³⁺ NPs plays an important role in the optical properties of this material, as mentioned before the pure GdVO₄ NPs show weak emission bands. The UV–Visible spectroscopy results show that GdVO₄:Dy³⁺ NPs absorb ultraviolet radiation and can be applied in DSSC as UV filter to prevent DSSC destruction under UV illumination. According to the PL spectroscopy results, GdVO₄:Dy³⁺ luminescent NPs can be applied in DSSC as DC material. In the present study, the use of GdVO₄:Dy³⁺ NPs thin film as DC layer lead to improved fill factor, current density and efficiency of DSSC. Use of a layer of GdVO₄:Dy³⁺ on the back surface of the PE cause the DSSC efficiency to increase by a factor of 2.64 % and with using it inside the PE this increase is 10.30 %. However, overuse of DC material reduces the efficiency of the DSSC.

Acknowledgments Authors are grateful to research council of the University of Kashan for providing financial support to undertake this work.

References

- H. Sun, L. Pan, Z. Piao, Z. Sun, Enhanced performance of cadmium selenide quantum dot-sensitized solar cells by incorporating long afterglow europium, dysprosium co-doped strontium aluminate phosphors. *J. Colloid Interface Sci.* **416**, 81–85 (2014)
- B. O'regan, M. Grätzel, Low cost and highly efficient solar cells based on the sensitization of colloidal titanium dioxide. *Nature* **335**(24), 737–740 (1991)
- M. Grätzel, Photoelectrochemical cells. *Nature* **414**(6861), 338–344 (2001)
- N. Sharifi, N. Ghazyani, N. Taghavinia, Morphological dependence of light backscattering from metallic back reflector films: application in dye-sensitized solar cells. *Phys. Status Solidi (a)* **212**(4), 785–790 (2015)
- K.H. Ko, Y.C. Lee, Y.J. Jung, Enhanced efficiency of dye-sensitized TiO₂ solar cells (DSSC) by doping of metal ions. *J. Colloid Interface Sci.* **283**(2), 482–487 (2005)
- A.S. Nair, R. Jose, V. Shengyuan, S. Ramakrishna, A simple recipe for an efficient TiO₂ nanofiber-based dye-sensitized solar cell. *J. Colloid Interface Sci.* **353**(1), 39–45 (2011)
- Q. Li, J. Lin, J. Wu, Z. Lan, Y. Wang, F. Peng, M. Huang, Enhancing photovoltaic performance of dye-sensitized solar cell by rare-earth doped oxide of Lu₂O₃:(Tm³⁺, Yb³⁺). *Electrochim. Acta* **56**, 4980–4984 (2011)
- K. Andreas, M. Grätzel, Dye-sensitized core-shell nanocrystals: improved efficiency of mesoporous tin oxide electrodes coated with a thin layer of an insulating oxide. *Chem. Mater.* **14**, 2930–2935 (2002)
- M. Zahedifar, Z. Chamanzadeh, S.M.H. Mashkani, Synthesis of LaVO₄:Dy³⁺ luminescent nanostructure and optimization of its performance as down-converter in dye-sensitized solar cells. *J. Lumin.* **135**, 66–73 (2013)
- C. Strümpel, M. McCann, G. Beaucarne, V. Arkhipov, A. Slaoui, V. Švrček, C. del Cañizo, I. Tobias, Modifying the solar spectrum to enhance silicon solar cell efficiency—an overview of available materials. *Sol. Energy Mater. Sol. Cells* **91**, 238–249 (2007)
- L. Guocong, D. Xuechen, L. Haibin, D. Hui, Z. Ligang, Novel polyhedron-like t-LaVO₄:Dy³⁺ nanocrystals: hydrothermal synthesis and PL properties. *Cryst. Growth* **310**, 4689 (2008)
- D.C. Yu, S. Ye, M.Y. Peng, Q.Y. Zhang, J.R. Qiu, J. Wang, L. Wondraczek, Efficient near-infrared downconversion in GdVO₄:Dy³⁺ phosphors for enhancing the photo-response of solar cells. *Sol. Energy Mater. Sol. Cells* **95**, 1590 (2011)
- C. Feng, J. Zhang, R. Lang, Z. Jin, Z. Wu, Z. Zhang, Unusual photo-induced adsorption–desorption behaviour of propylene on Ag/TiO₂ nanotube under visible light irradiation. *Appl. Surf. Sci.* **257**, 1864 (2011)
- T. Gavrilović, D.J. Jovanovic, V. Lujpur, M.D. Dramicanin, Multifunctional Eu³⁺-and Er³⁺/Yb³⁺-doped GdVO₄ nanoparticles synthesized by reverse micelle method. *Sci. Rep.* **4**, 4290 (2014)
- Y. Zheng, H. You, G. Jia, K. Liu, Y. Song, M. Yang, H. Zhang, Facile hydrothermal synthesis and luminescent properties of large-scale GdVO₄:Eu³⁺ nanowires. *Cryst. Growth Des.* **9**, 5101–5107 (2009)
- L. Yang, G. Li, M. Zhao, J. Zheng, X. Guan, L. Li, Morphology-controllable growth of GdVO₄:Eu³⁺ nano/microstructures for an optimum red luminescence. *Nanotechnology* **23**, 245602 (2012)
- J. Wang, Y. Xu, M. Hojamberdiev, J. Peng, G. Zhu, Na₂ EDTA-assisted hydrothermal synthesis and luminescent properties of YVO₄:Eu³⁺ with different morphologies in a wide pH range. *Mater. Sci. Eng. B* **156**, 42 (2009)
- L.-N. Jin, Q. Liu, W.-Y. Sun, Synthesis and photoluminescence of octahedral GdVO₄ microcrystals by hydrothermal conversion of Gd₂(CO₃)₃·xH₂O nanospheres. *Solid State Sci.* **19**, 45–50 (2013)
- A. De Vos, A. Szymanska, V. Badescu, Modelling of solar cells with down-conversion of high energy photons, anti-reflection coatings and light trapping. *Energy Convers. Manag.* **50**, 328–336 (2009)
- H. Cui, Y. Feng, W. Ren, T. Zeng, H. Lv, Y. Pan, Strategies of large scale synthesis of monodisperse nanoparticles. *Recent Pat. Nanotechnol.* **3**, 32–41 (2009)
- C.R. Ronda, Phosphors for lamps and displays: an applicational view. *J. Alloys Compd.* **225**, 534–538 (2005)
- J. Callaway, *Quantum theory of the solid state* (Academic Press, London, 1974)
- M.N. Kamalasanan, N.D. Kumar, S. Chandra, Structural, optical, and dielectric properties of sol-gel derived SrTiO₃ thin films. *J. Appl. Phys.* **74**, 679–686 (1993)
- X.-C. Jiang, L.-D. Sun, C.-H. Yan, Ordered nanosheet-based YBO₃:Eu³⁺ assemblies: synthesis and tunable luminescent properties. *J. Phys. Chem. B* **108**, 3387–3390 (2004)

25. B.M. van der Ende, L. Aarts, A. Meijerink, Lanthanide ions as spectral converters for solar cells. *J. Phys. Chem. Chem. Phys.* **11**, 11081–11095 (2009)
26. J. Liu, Q. Yao, Y. Li, Effects of downconversion luminescent film in dye-sensitized solar cells. *Appl. Phys. Lett.* **88**, 173119 (2006)
27. H. Hafez, J.H. Wu, Z. Lan, Q.H. Li, G.X. Xie, J.M. Lin, M.L. Huang, Y.F. Huang, M.S. Abdel-Mottaleb, Enhancing the photoelectrical performance of dye-sensitized solar cells using TiO₂:Eu³⁺ nanorods. *Nanotechnology* **21**, 415201 (2010)